한국지반환경공학회 논문집 제7권 제6호 2006년 12월 pp. 133~143

Numerical Modeling of Soil Liquefaction at Slope Site

사면에서 발생하는 액상화 수치해석

Park, Sungsik*
박 성 식*

Abstract

A fully coupled effective stress dynamic analysis procedure for modeling seismic liquefaction on slope is presented. An elasto-plastic formulation is used for the constitutive model UBCSAND in which the yield loci are radial lines of constant stress ratio and the flow rule is non-associated. This is incorporated into the 2D version of Fast Lagrangian Analysis of Continua (FLAC) by modifying the existing Mohr-Coulomb model. This numerical procedure is used to simulate centrifuge test data from the Rensselaer Polytechnic Institute (RPI). UBCSAND is first calibrated to cyclic direct simple shear tests performed on Nevada sand. Both pre- and post-liquefaction behaviour is captured. The centrifuge test is then modeled and the predicted accelerations, excess porewater pressures, and displacements are compared with the measurements. The results are shown to be in general agreement. The procedure is currently being used in the design of liquefaction remediation measures for a number of dam, bridge, tunnel, and pipeline projects in Western Canada.

Keywords : Liquefaction, Slope, UBCSAND, Centrifuge test, Direct simple shear

요 지

본 논문에서는 저자가 제안한 유효응력모델을 이용하여 지진시 사면의 동적거동에 관한 수치해석을 수행하였다. 항복함수는 동일한 응력비를 가진 무한개의 방사선을 의미하며, 비관련 유동규칙을 가진 탄소성모델인 UBCSAND를 이용하였다. 이 모델은 FLAC내에 내장된 Mohr-Coulomb모델을 변형한 형태이다. UBCSAND모델을 이용하여 RPI에서 수행한 원심모형실험결과를 예측하였다. 먼저, UBCSAND모델을 Nevada모래를 사용한 반복 직접단순전단시험결과를 이용하여 검증하였으며, 액상화전후의 거동을 예측하였다. 이와 같이 검증된 모델을 원심모형실험에서 계측된 가속도, 과잉간극수압, 변위와 서로 비교하였다. 일반적으로 계측치와 예측치가 일치하였다. 유효응력모델을 이용한 동적 수치해석기법은 서부 캐나다에서 댐, 교량, 터널, 파이프라인과 관련된 액상화 프로젝트에 실제 사용되고 있다.

주요어 : 액상화, 사면, UBCSAND, 원심모형실험, 직접단순전단

1. Introduction

Displacements arising from seismic liquefaction and slope failure due to heavy rainfall can be very large (Kim et al., 2004) and are a major concern for earth structures located in regions of moderate to high seismicity. Liquefaction is caused by high porewater pressures resulting from the tendency for granular soils to compact when subjected to cyclic loading. Remedial measures typically involve attempts to prevent or curtail liquefaction so that displacements are reduced to tolerable levels. Modifications can also be made to the structure so that larger displacements can be

* Member, Post-Doctoral Researcher, Dept. of Civil Engrg., Kyungpook National Univ.(E-mail : park1059@hanmail.net)

tolerated. In either case, the rational design for remediation requires a reliable prediction of soil-structure response during the design earthquake.

State-of-practice procedures for evaluating liquefaction typically use separate analyses for liquefaction triggering (e.g. Youd et al., 2001), flow slide (limit equilibrium with residual strength), and displacements (Newmark sliding block). Yoo et al. (2005) used a Geographic Information System (GIS) to evaluate the liquefaction potential of silty sand. While the results of the triggering evaluation are used as input into the flow slide and displacement evaluations, the analyses are otherwise independent. While this practice often provides a good screening level tool, these simplified total stress analyses cannot reliably predict excess porewater pressures, accelerations, or displacement patterns.

State-of-the-art procedures involve dynamic finite element or finite difference analyses using effective stress procedures coupled with fluid flow predictions. These analyses can estimate the displacements, accelerations and porewater pressures caused by a specified input motion. Triggering of liquefaction, displacements and flow slide potential are addressed in a single analysis. Such analyses involve capturing the liquefaction behaviour of a soil element as observed in laboratory tests, and then modeling the soil-structure as a collection of such elements subjected to the design earthquake base motion.

It is vital that these sophisticated procedures be verified before they are used in practice. Instrumented centrifuge model tests can be used for verification and have some advantages over observed field behaviour. Centrifuge tests allow the measurement of displacements, input and induced accelerations, and porewater pressures under field stress conditions. These tests can therefore provide a useful database for verification of numerical modeling. This approach is used below.

2. Liquefaction

Liquefaction is caused by the tendency of granular soil to contract when subjected to monotonic or cyclic shear loading. When this contraction is prevented or curtailed by the presence of water in the pores, normal stress is transferred from the soil skeleton to the water. This can cause high excess pore pressures resulting in a very large reduction in shear stiffness. Large shear strains may occur, and the soil will dilate with these strains unless the soil is very loose. This dilation causes the porewater pressure to drop and the stiffness to increase which can limit the strains induced by a load cycle. This behaviour is illustrated in Figure 1 for monotonic loading.

It is this tendency of the soil skeleton to

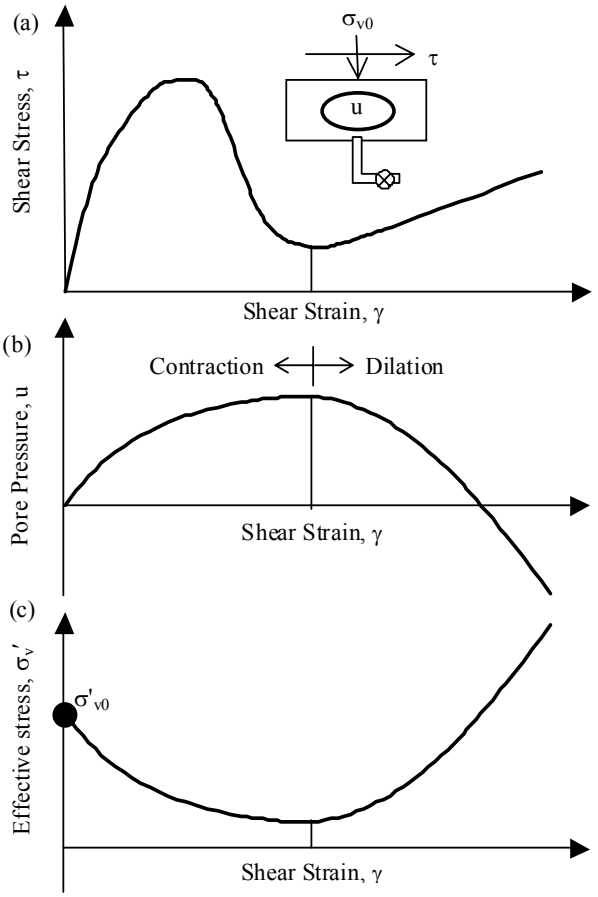

Fig. 1. Undrained response of loose sand in simple shear: (a) stress-strain, (b) pore pressure, and (c) effective stress response

contract and dilate that controls its liquefaction response. Once the skeleton behaviour is modeled, the response under drained, undrained or coupled stress-flow conditions can be computed by incorporating the bulk stiffness and flow of the pore fluid.

3. Constitutive Model: UBCSAND

The simplest realistic model for soil is the classic Mohr-Coulomb elastic-plastic model as depicted in Figure 2. Soils are modeled as elastic below the strength envelope and plastic on the strength envelope with plastic shear and volumetric strains increments related by the dilation angle, ψ_m. This model is really too simple for soils since plastic strains also occur for stress states below the strength envelope. The UBCSAND stress-strain model described herein modifies the Mohr-Coulomb model incorporated in FLAC (Itasca, 2000) to capture the plastic strains that occur at all stages of loading. Yield loci are assumed to be radial line of constant stress ratio as shown in Figure 3. Unloading is assumed to be elastic. Reloading induces plastic response but with a stiffened plastic shear modulus.

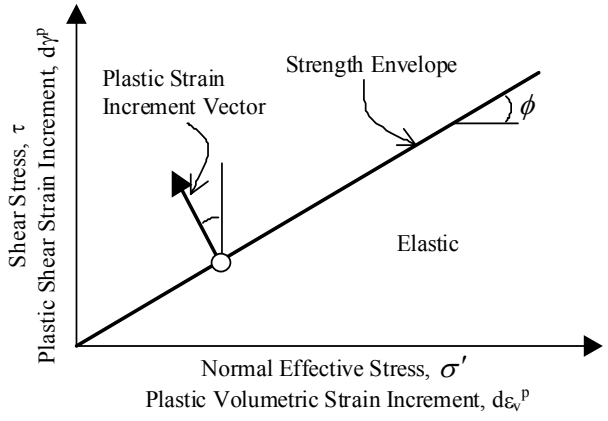

Fig. 2. Classic Mohr-Coulomb model

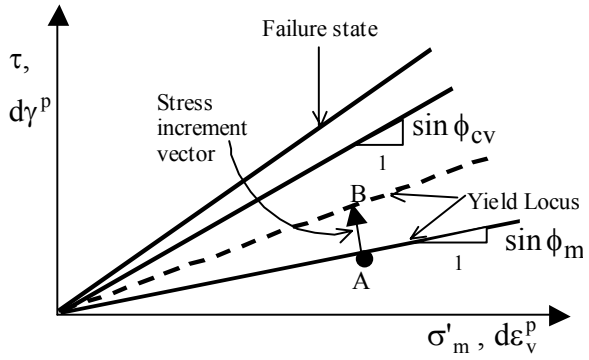

Fig. 3. UBCSAND model

The plastic shear modulus relates the shear stress and the plastic shear strain and is assumed to be hyperbolic with stress ratio as shown in Figure 4. Moving the yield locus from A to B in Figure 3 requires a plastic shear strain increment, $d\gamma^P$, as shown in Figure 4, and is controlled by the plastic shear modulus, G^P. The associated plastic volumetric strain increment, $d\varepsilon_v^P$, is obtained from the dilation angle ψ_m:

$$d\varepsilon_v^P = d\gamma^P \cdot \sin\psi_m \qquad (1)$$

The dilation angle is based on laboratory data and energy considerations and is approximated by

$$\sin\psi_m = \sin\phi_m - \sin\phi_{cv} \qquad (2)$$

where ϕ_{cv} is the phase transformation or constant volume friction angle and ϕ_m describes the current yield locus. A negative value of ψ_m corresponds to contraction. Contraction occurs for stress states

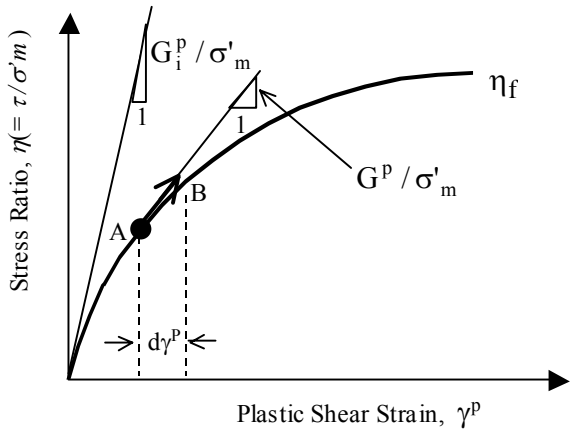

Fig. 4. Hyperbolic stress-strain relationship

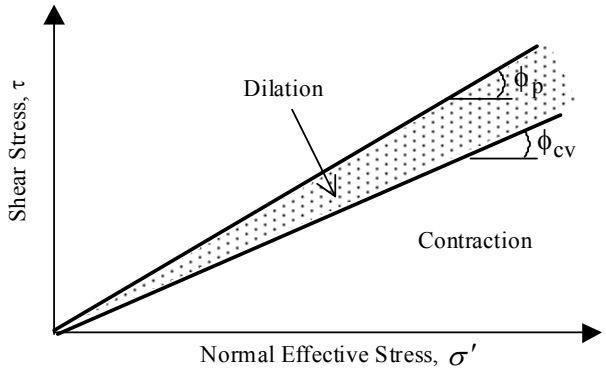

Fig. 5. Zones of shear-induced contraction and dilation

below ϕ_{cv} and dilation above as shown in Figure 5. Additional information on UBCSAND is presented by Park et al. (2005).

Elastic and plastic properties for the model are defined as follows.

3.1 Elastic Properties

The elastic bulk modulus, B, and shear modulus, G, are assumed to be isotropic and stress level dependent. They are described by the following relations where k_G^e is modulus number, P_a is atmospheric pressure, σ'_m is the mean effective stress, and a α (=2(1+ν)/(1−2ν)/3) depends on the Poisson's ratio:

$$G = k_G^{\,e} \cdot P_a \cdot \left(\frac{\sigma'_m}{P_a} \right)^{0.5} \tag{3}$$

$$B = \alpha \cdot G \tag{4}$$

3.2 Plastic Properties

The plastic properties used by the model are the peak friction angle ϕ_P, the constant volume friction angle ϕ_{cv}, and plastic shear modulus G^P, where

$$G^P = G_i^P \cdot \left(1 - \frac{\eta}{\eta_f} R_f \right)^2 \tag{5}$$

where $G_i^p = k_G^p \cdot P_a \cdot (\sigma'_m/P_a)^{0.4}$ and $k_G^p \approx 8 \cdot (D_r)^4 \cdot k_G^p + 100$, η is the current stress ratio ($=\tau/\sigma'_m$), η_f is the stress ratio at failure, R_f is the failure ratio used to truncate the hyperbolic relationship, and D_r is a relative density.

The position of the yield locus ϕ_m is known for each element at the start of each time step. If the stress ratio increases and plastic strain is predicted, then the yield locus for that element is pushed up by an amount $d\phi_m$ as given by Equation 6. Unloading of stress ratio is considered to be elastic. Upon reloading, the yield locus is set to the stress ratio corresponding to the stress reversal point.

$$d\phi_m = \left(\frac{G^P}{\sigma'_m} \right) \cdot d\gamma^P \tag{6}$$

The elastic and plastic parameters are highly dependent on relative density, which must be considered in any model calibration. These parameters can be selected by calibration to laboratory test data. The response of the model can also be compared to a considerable database for triggering of liquefaction under earthquake loading in the field. This database exists in terms of penetration resistance, typically from cone penetration (CPT) or standard penetration (SPT) tests. A common relationship between $(N_1)_{60}$ values from the SPT and the cyclic stress ratio that triggers liquefaction for a magnitude 7.5 earthquake is given by Youd et al. (2001). Comparing laboratory data based on relative density to field data based on penetration resistance relies upon an approximate conversion, such as that proposed by Skempton (1986):

$$35 < \frac{(N_1)_{60}}{D_r^{\,2}} < 60 \tag{7}$$

Model parameters based on penetration resistance and field observation may be useful for field

conditions where it is very difficult to retrieve and test a representative sample. However, this indirect method is not appropriate for simulation of centrifuge models. Calibrations for this case should be based on direct laboratory testing of samples that are prepared in the same manner as the centrifuge model.

4. Simulation of Cyclic Element Test Data

A number of cyclic direct simple shear tests have been conducted on Fraser River sand at the University of British Columbia. The samples were prepared by air pluviation with a target relative density D_r of 40% and tested at an initial vertical effective stress, σ'_{vo}, of 100 kPa. Samples were also tested at σ'_{vo} of 200 kPa with a D_r of 44%. Samples were subjected to cyclic shear under constant volume conditions that simulate undrained response at a range of cyclic stress ratios (CSR). Typical examples of measured response are shown in Figures 6 and 7. From Figure 6a it may be seen that as the shear stress is cycled, the effective stress decreases as the pore pressure increases. The ratio r_u is given by $(u - u_0) / \sigma'_{v0}$, where u_0 and u are the initial and current pore pressures. r_u approaches unity after 5 cycles, which corresponds to a state of zero effective stress. Application of further cycles produces very large shear strains in the range of 10 to 15% or more as shown in Figure 6b. However, the strain per cycle is limited as the pore pressures drop with strain due to dilation.

Figures 6 and 7 also show the response predicted using UBCSAND. The elastic and plastic parameters selected by the calibration were the same for both tests. The model gives a reasonable represen-tation of the observed response, although the final predicted strains are less than measured for Figure 6. A summary of the test results and the UBCSAND calibration are shown in Figure 8. The predicted and measured liquefaction response for σ'_{vo} of 100 and 200 kPa is in close agreement.

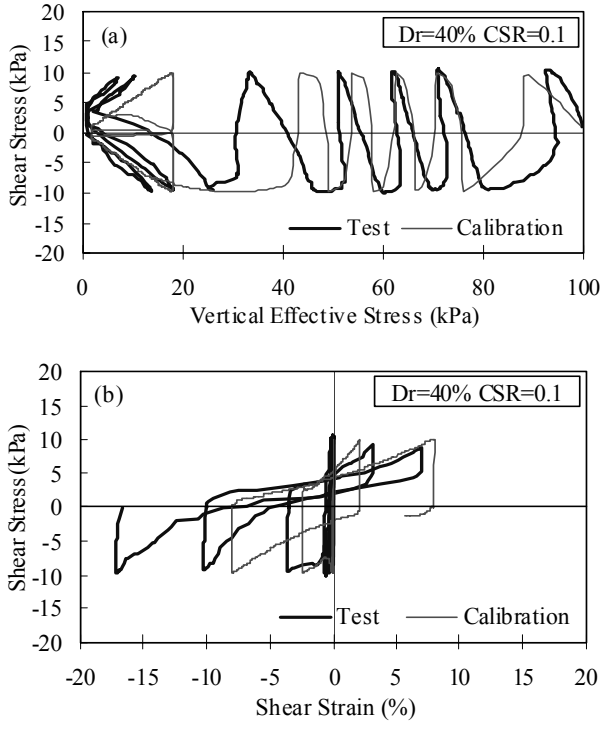

Fig. 6. Stress path and stress-strain relationship (CSR=0.1)

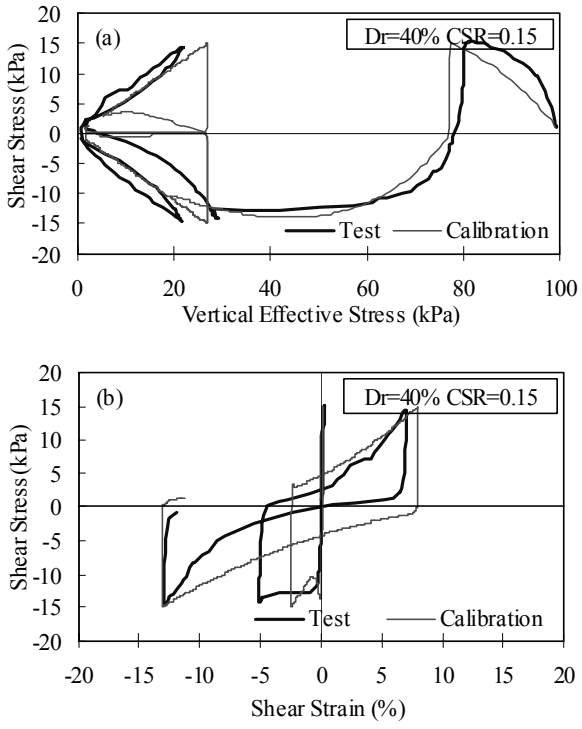

Fig. 7. Stress path and stress-strain relationship (CSR=0.15)

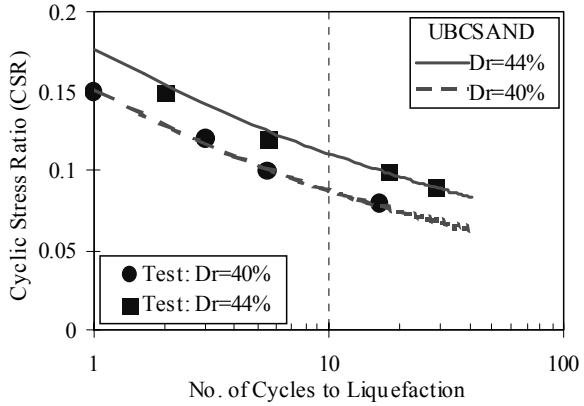

Fig. 8. Predicted and measured liquefaction response of Fraser River sand

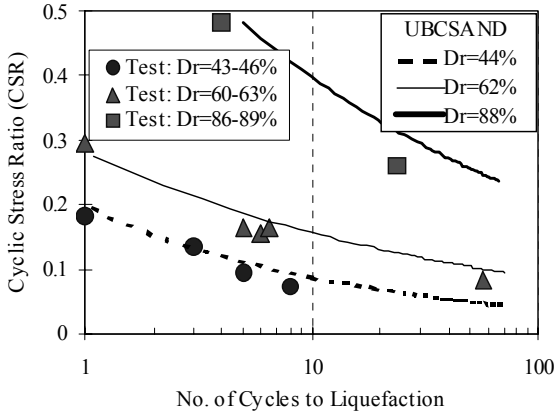

Fig. 9. Liquefaction resistance of Nevada sand

5. Centrifuge Test

A simulation using UBCSAND was made of a centrifuge test carried out at RPI as described in Table 1. In the centrifuge test, a small model is used that is subjected to a high acceleration field during the test. This has the effect of increasing its stresses by the ratio of the induced acceleration divided by the acceleration of gravity. This ratio (centrifuge acceleration) is 60 for this centrifuge model as indicated by Table 1. The centrifuge model under the increased acceleration field can also be thought of as representing a prototype that is 60 times larger than the actual model. Results from the centrifuge test can be presented at either the model or prototype scale. The prototype scale is used for this paper.

While in flight, a motion simulating an earthquake time history is applied to the base of the model. For dynamic similitude at the model scale, the earthquake time scale must be decreased by a factor of 60, and the earthquake acceleration increased by the same factor. The engineering coefficient of permeability k will also increase by this same factor due to the increased unit weight of the fluid. k should be decreased for hydraulic similitude, although it is not necessary to model a specific k. The water/metulose solution with 60 times the viscosity of water is used to prevent rapid rates of dissipation that might unduly curtail liquefaction effects.

Nevada sand was used for this centrifuge test and its liquefaction and permeability (at 1g using water as pore fluid) properties were obtained from laboratory tests (Arulmoli et al., 1992; Kammerer et al., 2000; Taboada-Urtuzuastegui et al., 2002). Its measured liquefaction resistance together with the UBCSAND prediction is shown in Figure 9.

5.1 Numerical Modeling of RPI Centrifuge Test

The cross section for RPI centrifuge test is shown in Figure 10 and comprises a steep 1.5:1 slope in loose fine sand with D_r = 40% (Taboada-Urtuzuastegui et al., 2002). The base motion consists of 20 cycles of 0.2 g at a frequency of 1 Hz. The container for centrifuge model was rigid and this was simulated in the FLAC model by

Table 1. RPI centrifuge model test

Test condition	Dr	Centrifuge Acceleration	Max. σ'_{vo}	Max. Soil depth	Fluid viscosity
Slope	40%	60 g	100 kPa	10 m	60μw[(i)]

(i) μw is a viscosity of water.

applying the input motion to the vertical sides as well as the base. The key inputs including water bulk stiffness (B_f) in the numerical model are listed in Table 2. Pore pressures and accelerations were measured away from the face of the slope, approximating free field conditions, as well as adjacent to the slope.

The predicted and observed accelerations and pore pressures in the free field are shown in Figures 11 and 12. As expected, similar trends are seen as for the level ground centrifuge test (Gonzalez et al., 2002), i.e. r_u of 100% and reduced accelerations.

The accelerations and pore pressures near the slope are shown in Figures 13 and 14. It may be seen in Figure 13 that there is little or no

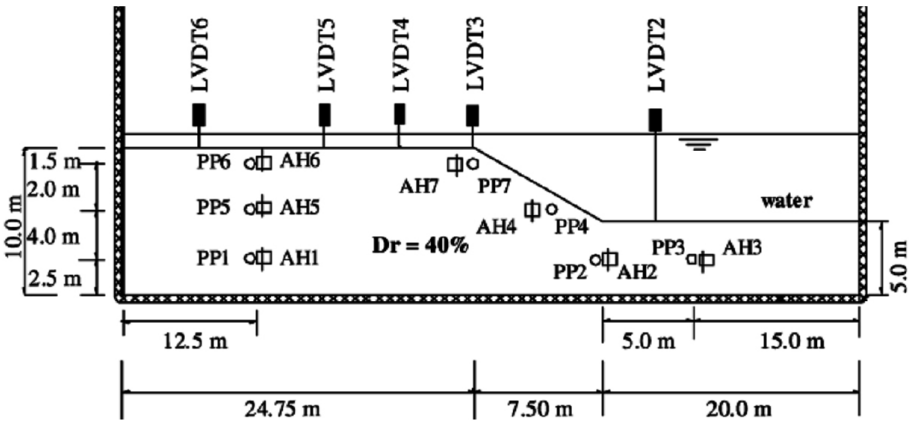

Fig. 10. Cross section of RPI centrifuge model (Taboada- Urtuzuastegui et al., 2002)

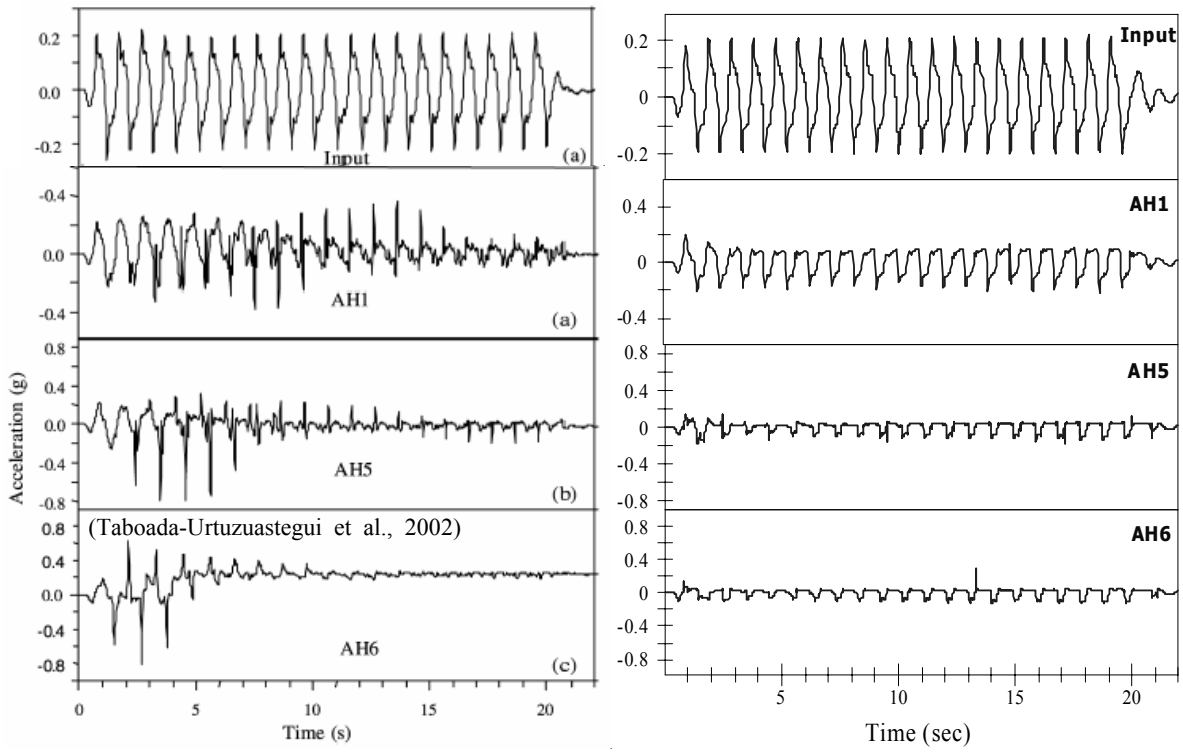

Fig. 11. Measured (left) and predicted (right) accelerations at free field

Table 2. Key input for numerical analysis

k_G^e	α	k_G^p	ϕ_{cv}	ϕ_p	R_f	B_f after spinup	Permeability
867	0.75	282	33°	34°	0.92	$1x10^5$ kPa	$2.1x10^{-5}$ m/sec

reduction in the accelerations. Instead, large upslope acceleration spikes occur. Excess pore pressures are shown in Figure 14. Large negative excess pore pressure spikes occur that coincide in time with the upslope acceleration spikes. The slope is steep and the upslope acceleration of the base tends to induce failure of the slope and relative downslope movement. The soil dilates as it shears in the downslope direction, producing negative pore pressures which stiffen the shear modulus. Enough strength is mobilized through this dilation to arrest the downslope movement

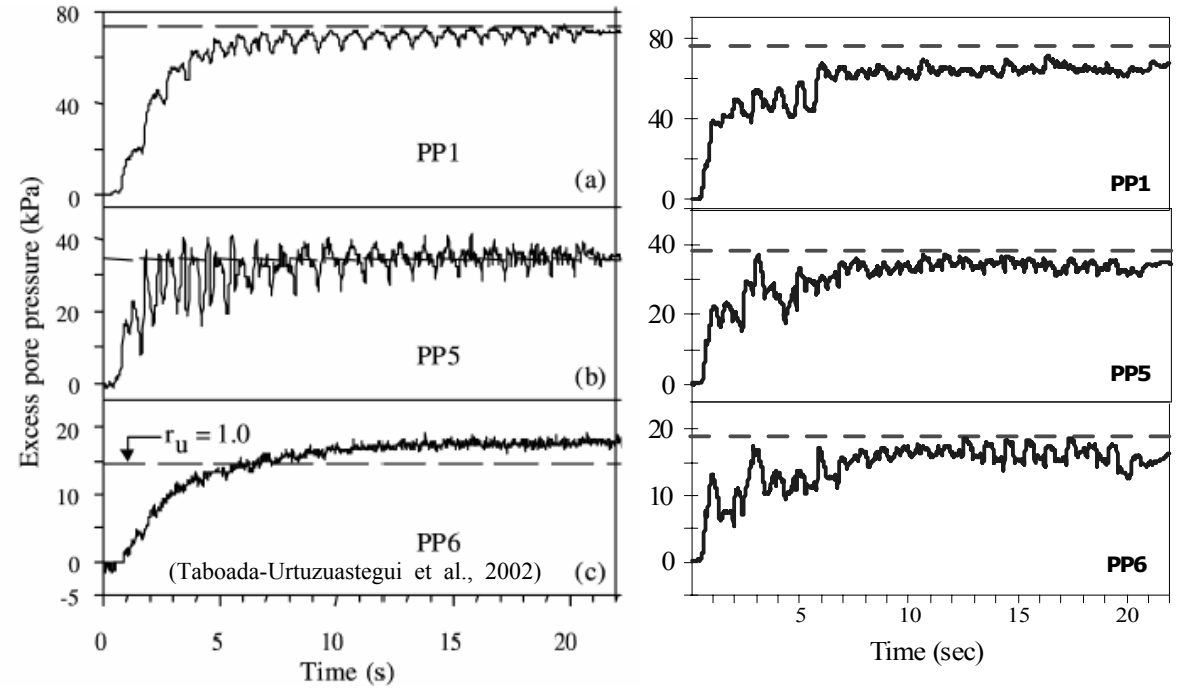

Fig. 12. Measured (left) and predicted (right) excess pore pressures at free field

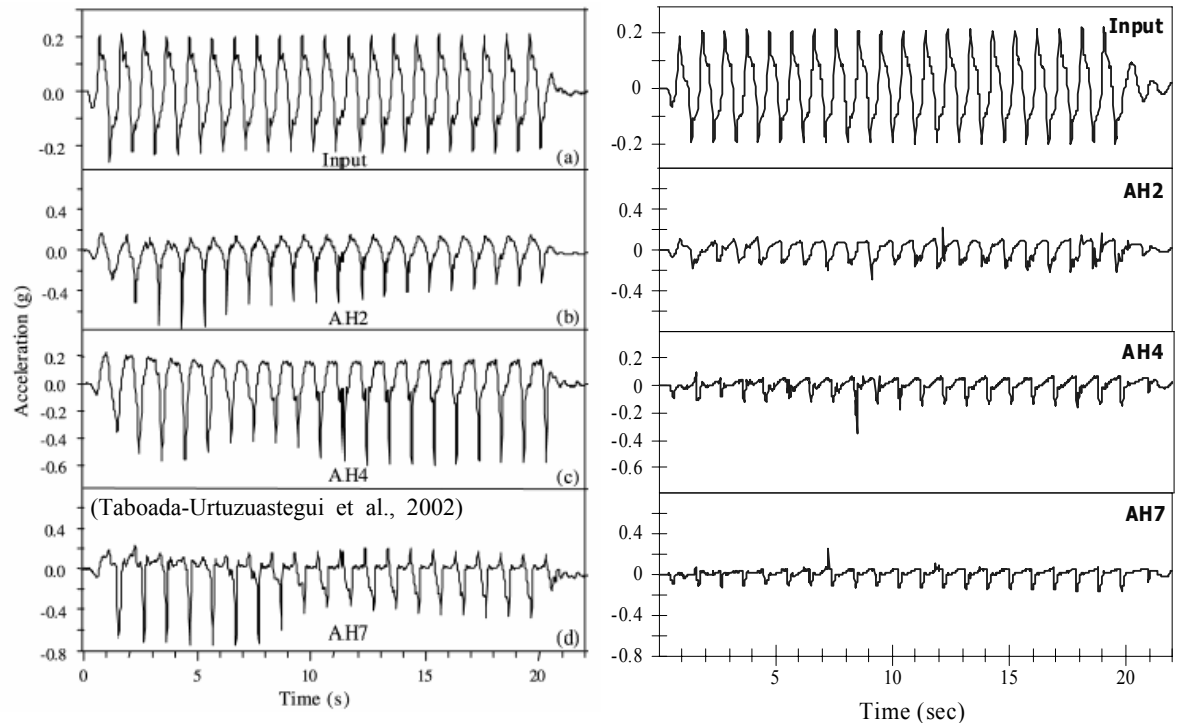

Fig. 13. Measured (left) and predicted (right) accelerations near the slope

and gives rise to the acceleration spike (Taboada-Urtuzuastegui et al., 2002).

UBCSAND provides a reasonable prediction of the accelerations and pore pressure response for the free field. More significant differences are observed for locations near the slope. Some of these differences are due to UBCSAND under predicting the dilative spikes. The measured and predicted displacements after shaking are shown in Figures 15 and 16. It may be seen that both

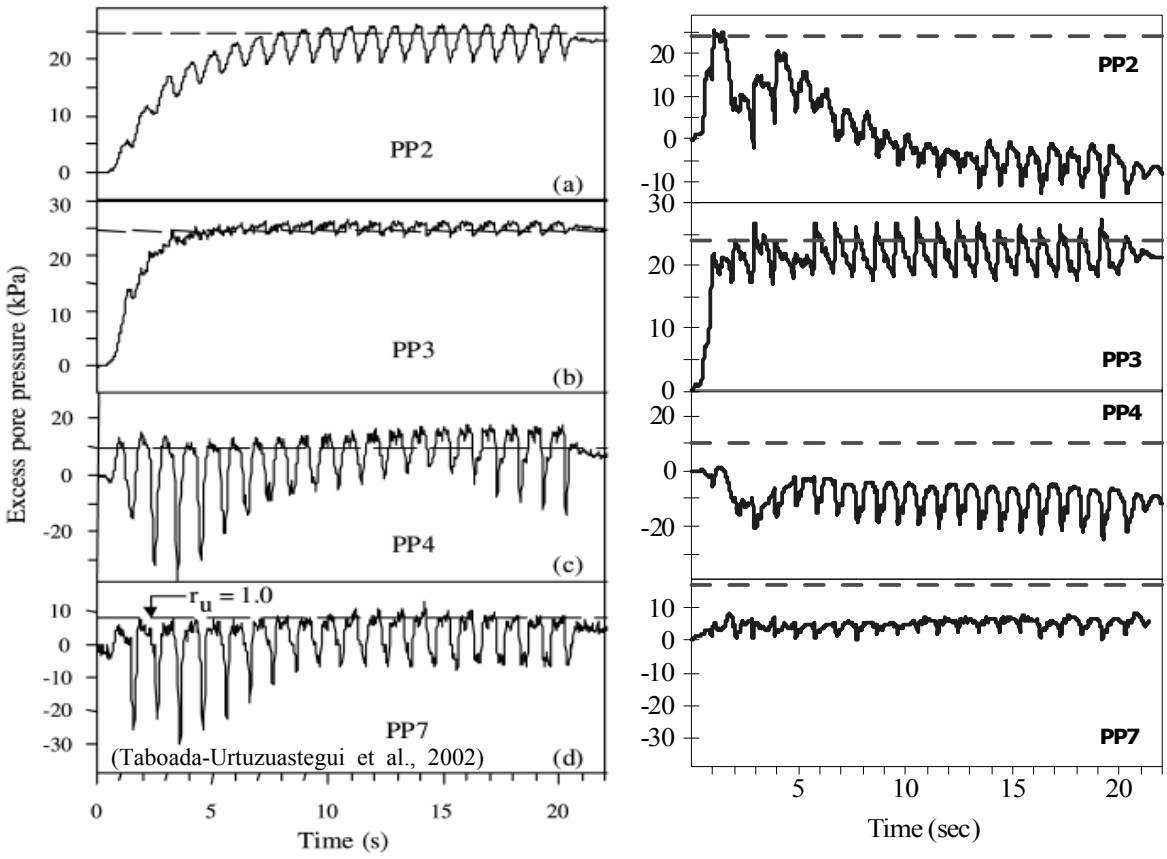

Fig. 14. Measured (left) and predicted (right) excess pore pressures near the slope

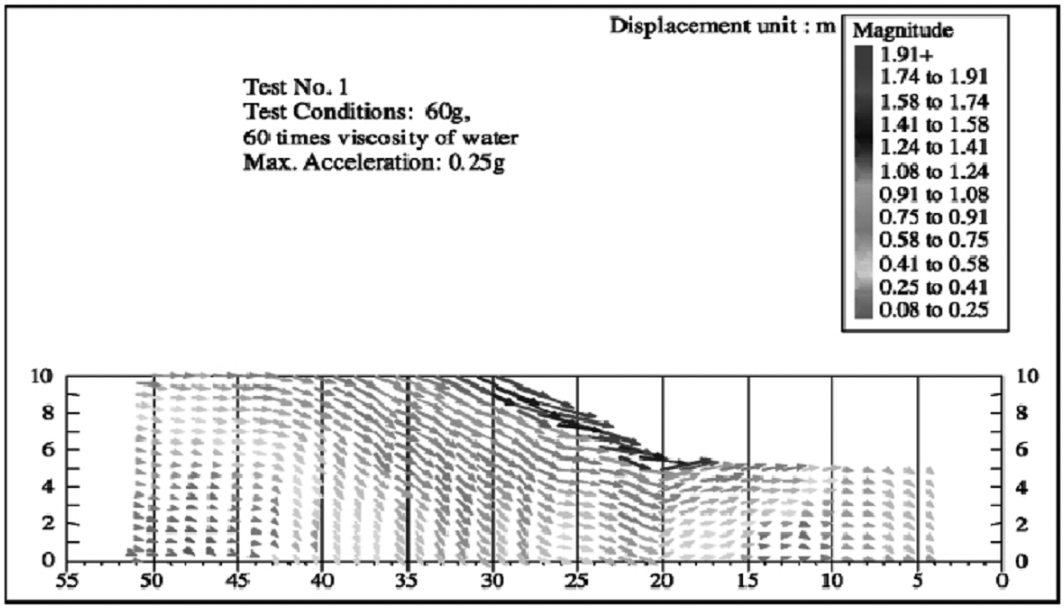

Fig. 15. Measured displacements (Taboada-Urtuzuastegui et al., 2002)

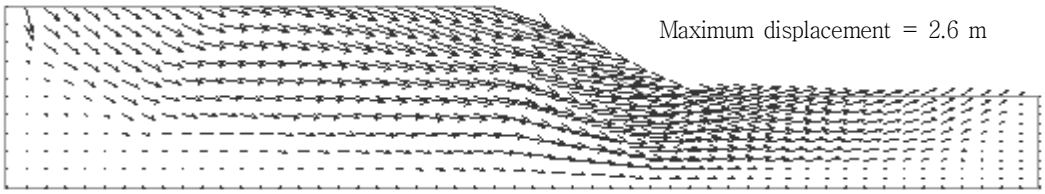

Fig. 16. Predicted displacements using UBCSAND

the magnitude and pattern of displacements are in general agreement.

In summary,

(a) UBCSAND provides reasonable agreement with RPI centrifuge test, although further study is needed for locations close to the sloping face,

(b) a decrease in accelerations after liquefaction was not observed near the slope,

(c) a large upslope acceleration spikes occurred near the slope,

(d) a decrease in pore pressure due to dilation corresponded with these upslope acceleration spikes, and,

(e) the dilative spikes prevented very large displacements from occurring in this homo-geneous fine sand model.

6. Summary

A fully coupled effective stress dynamic analysis procedure has been presented. The procedure is first calibrated by comparison with laboratory element test data and then verified by comparison with a centrifuge model test.

RPI centrifuge model represented a steep slope condition in homogeneous loose fine sand. The results showed that large upslope acceleration spikes occurred near the face of the slope after liquefaction. These acceleration spikes corresponded with large negative excess pore pressure spikes associated with dilation. It is the increase in effective stress associated with these negative pore pressure spikes that curtails the displacements and makes the slope more stable than might be expected under cyclic loading. The overall pattern of predicted response is in reasonable agreement with the measurements, although both the accele-ration and pore pressure spikes are under predicted by the UBCSAND analysis.

ACKNOWLEDGMENT

This work was partially supported by the Brain Korea 21 Project in 2006.

(접수일 : 2006. 10. 2 심사일 : 2006. 10. 12 심사완료일 : 2006. 10. 31)

REFERENCES

1. Arulmoli, K., Muraleetharan, K.K., Hossain, M.M. and Fruth, L.S.(1992), VELACS laboratory testing program, soil data report. The Earth Technology Corporation, Irvine, California, Report to the National Science Foundation, Washington D.C., March.Beaty, M. & Byrne, P. 1998. An effective stress model for predicting liquefaction behaviour of sand, *ASCE Geotechnical Special Publication*, No. 75, pp. 766~777.
2. Gonzalez, L, Abdoun, T. and Sharp, M.K.(2002), Modeling of seismically induced liquefaction under high confining stress, *International Journal of Physical Modelling in Geomechanics*, Vol. 2, No. 3, pp. 1~15.
3. Itasca(2000), FLAC, version 4.0. Itasca Consulting Group Inc., Minneapolis.

4. Kammerer, A., Wu, J., Pestana, J., Riemer, M. and Seed, R.(2000), Cyclic simple shear testing of Nevada sand for PEER Center project 2051999. *Geotechnical Engineering Research Report* No. UCB/GT/00-01, University of California, Berkeley, January.
5. Kim, Y.M., Park, H.K. and Choi, M.H.(2004), Instability analysis of road landfill slope during heavy rainfall, *Journal of Korean Geo-environmental Society*, Vol. 5, No. 3, pp. 41~50.
6. Park, S.S., Kim, Y.S., Byrne, P.M. and Kim, D.M.(2005), A simple constitutive model for soil liquefaction analysis, *Journal of Korean Geotechnical Society*, Vol. 21, No. 8, pp. 27~35.
7. Skempton, A.W.(1986), Standard penetration test procedures and the effects in sands of overburden pressure, relative density, particle size, ageing and overconsolidation, *Geotechnique*, Vol. 36, No. 3, pp. 425~447.
8. Taboada-Urtuzuastegui, V.M., Martinez-Ramirez, G. and Abdoun, T.(2002), Centrifuge modeling of seismic behavior of a slope in liquefiable soil, *Soil Dynamic and Earthquake Engineering*, Vol. 22, pp. 1043~1049.
9. Yoo, S.D., Kim, H.T., Song, B.W. and Lee, H.K.(2005), Assessment of liquefaction potential on non-plastic silty sand layers using geographic information system(GIS) and Standard Penetration Test results, *Journal of Korean Geo-environmental Society*, Vol. 6, No. 2, pp. 5~14.
10. Youd, T.L., Idriss, I. M., Andrus, R.D., Arango, I., Castro, G., Christian, J.T., Dobry, R., Finn, W.D.L., Harder Jr., L.F., Hynes, M.E., Ishihara, K., Koester, J.P., Liao, S., Marcuson III, W.F., Martin, G.R., Mitchell, J.K., Moriwaki, Y., Power, M.S., Robertson, P.K., Seed, R.B. and Stokoe, K.H.(2001), Liquefaction Resistance of Soils: Summary Report from the 1996 NCEER and 1998 NCEER/NSF Workshops on Evaluation of Liquefaction Resistance of Soils, *Journal of Geotechnical and Geoenvironmental Engineering*, Vol. 127, No. 10, pp. 817~833.